

## Analysis of Al nanocrystals nucleation process in AlNiGd metallic glass during annealing and severe plastic deformation

© E.A. Sviridova,<sup>1,2</sup> S.V. Vasiliev,<sup>1,2</sup> G.E. Abrosimova,<sup>3</sup> V.I. Tkatch<sup>1</sup>

<sup>1</sup>A.A. Galkin Donetsk Institute for Physics and Engineering,  
283048 Donetsk, Russia

<sup>2</sup>Donbass National Academy of Civil Engineering and Architecture,  
286123 Makeyevka, Russia

<sup>3</sup>Osipyan Institute of Solid State Physics RAS Russian Academy of Sciences,  
142432 Chernogolovka, Moscow District, Russia  
e-mail: ksvir@list.ru

Received November 21, 2023

Revised December 24, 2023

Accepted December 25, 2023

Analysis of the process of nanocomposite structures formation in Al<sub>87</sub>Ni<sub>8</sub>Gd<sub>5</sub> metallic glass under isothermal annealing at 448 K and under high pressure torsion straining was performed in the frames of the classical equation for rate of homogeneous nucleation. The value of specific free energy of the nucleus/matrix interface, which agreed with the experimentally established volume density of nanocrystals, was used as the only one free parameter. The nucleation rate during annealing was estimated using the effective diffusion coefficient, which was taken from the literature, while in the equation for deformation-induced nucleation rate the value of the diffusion coefficient determined by the size of nanocrystals in the deformed sample was used. It was established that approach proposed in this work, which consisted in substituting into the equation for nucleation rate during deformation the value of the work of critical nucleus formation corresponding to room temperature, correctly described the experimentally established enhanced volume density of nanocrystals in deformed samples.

**Keywords:** metallic glass, annealing, deformation, nanocomposite, density of nanocrystals, nucleation rate.

DOI: 10.21883/0000000000

### Introduction

Metallic alloys with an amorphous –nanocrystalline structure (nanocrystals with dimensions  $\leq 30$  nm and density  $\geq 10^{21}$  m<sup>-3</sup>, dispersed in an amorphous matrix), synthesized at the end of the last century [1,2], have now become a promising class materials with unique complexes of physical properties. The main methods for obtaining nanocomposite structures are incomplete amorphization of the solidifying melt [2] and partial crystallization of the amorphous phase during heating [1,3] or in process of deformation [4]. In view that the properties of nanophase composites depend on structural parameters (the size of nanocrystals and their volume fraction) [5], the values of which are determined by the synthesis modes, the most common method for their preparation is the controlled crystallization of amorphous phases.

Obviously, due to a number of physical and technical reasons, heat treatment (isothermal holding or heating at a constant rate) is a more convenient method, because it allows to realize a wide range of structural states using well established technological solutions. However, nanocrystallization during annealing is accompanied by an almost complete loss of plasticity [6–8], which significantly limits the usage value of nanophase composites formed by heat treatment. In contrast to the heat-treated materials, those materials with nanocomposite structures obtained

in the process of severe plastic deformation retain an acceptable level of plasticity [9,10], which is caused by the increased concentration of free volume [11,12] and is of interest with from a practical point of view.

Another characteristic feature of the structure of deformation-induced nanocomposites is significantly (in 2–4 times) smaller sizes of nanocrystals and their higher (by 1–2 orders) volume density than those in the heat-treated samples [13,14]. Despite the undoubtedly fundamental interest and practical importance of the materials with a nanocomposite structure, the regularities of the process of deformation-induced crystallization and, in particular, the nucleation process remain a subject of discussion [15].

Until now, the theoretical basis for the analysis of crystallization processes of glasses is the classical theory of crystallization which is a set of equations developed [16] by the middle of the last century that describe the temperature-time dependences of the rates of nucleation and growth of crystals and the kinetics of transformation. Despite the fact that most of these equations were derived for small deviations from equilibrium, subsequent practice has shown that, with certain modifications, the classical theory correctly describes the crystallization processes of glasses [17,18], including the formation of nanocomposite structures with a high density of nanocrystals at heating or isothermal annealing [19–22]. However, for deformation-induced crystallization of this kind there is no quantitative

description due to the complex nature of the processes, which limits the correct estimation of the parameters.

There is no doubt that one of the most important parameters determining the rate of nucleation and growth of crystals is the diffusion coefficient at the interface between the parent and crystalline phases. The nature of this type of diffusion, called effective one, differs from the processes of self- and heterodiffusion (migration) of atoms, and the values of its coefficients ( $D_{\text{eff}}$ ) are determined by comparing model calculations with the experimentally measured parameters of the crystallization process [23]. In particular, to characterize the process of deformation-induced crystallization in the high-pressure torsion (HPT) method, it was recently proposed [24,25] to use the value of the diffusion coefficient determined from the particle sizes of the new phase. Calculated in these studies in the frames of the parabolic growth equation [26] from the average grain sizes  $L$  that grew during deformation in the time  $t$ , values of  $D_{\text{eff}}$  for crystals of the solid solution of tin in copper and for  $\alpha$ -Fe nanocrystals in glasses based on iron turned out to be several orders of magnitude higher than the heterodiffusion coefficients of the components of these alloys at room temperature. Based on the estimates obtained, a conclusion was made about the analogy of the processes of thermal diffusion and mass transfer stimulated by deformation, and the concept of the effective temperature of the deformation process was introduced, which is significantly higher than room temperature [24,27].

Accounting that the processes of crystal nucleation and growth are diffusion-controlled, it seems interesting to use the  $D_{\text{eff}}$  values as a parameter to estimate the rate of nucleation of Al nanocrystals in the process of deformation-induced crystallization. Metallic glass  $\text{Al}_{87}\text{Ni}_8\text{Gd}_5$  was chosen as the object of analysis, the structural parameters of the nanocomposite states of which were determined both after isothermal annealing and after deformation by the HPT method.

## 1. Materials and experimental procedure

The starting material for the formation of nanocomposite structures was an amorphous ribbon with a thickness of  $69\ \mu\text{m}$  and a width of 10 mm, obtained by spinning a melt of the nominal composition  $\text{Al}_{87}\text{Ni}_8\text{Gd}_5$  on a bronze quenching wheel [23]. Isothermal annealing of the ribbon sample was carried out in a flow of argon in a resistance furnace, preheated to the required temperature (448 K). The holding time was 3600 s. The deformation of the samples was carried out by torsion at a speed of 1 rpm between Bridgman anvils under pressure (HPT)  $P = 4\ \text{GPa}$  at room temperature. The deformed samples had the shape of disks with a diameter of 10 mm.

The structures of heat-treated and deformed samples were studied by X-ray diffraction using a Siemens D-500 diffractometer with Co  $K_{\alpha}$ -radiation. To estimate

the structural parameters of nanophase composites (sizes of nanocrystals and their volume fraction) formed during processing, contributions from the amorphous and nanocrystalline phases were identified in the diffraction patterns. The sizes of nanocrystals,  $L$ , were estimated from the half-width of the diffraction line (111),  $\Delta\beta$ , using the well-known Selyakov–Scherrer formula [28]:

$$L = \lambda / (\Delta\beta \cos \theta), \quad (1)$$

where  $\lambda$  is the radiation wavelength,  $\theta$  is the reflection angle. The  $\Delta\beta$  value was determined taking into account the instrumental contribution to the broadening. The volume fraction of the crystalline phase was calculated from the ratio of the integral intensity of the peaks of the crystalline phase to the total intensity of scattered radiation from the relation [29]

$$X = I_{\text{cr}} / (I_{\text{am}} + \alpha I_{\text{cr}}), \quad (2)$$

where  $I_{\text{cr}}$  and  $I_{\text{am}}$  are the integral intensities of reflections from the crystalline and amorphous phases (in the angular range under study), respectively, and  $\alpha$  is a parameter that takes into account the differences in the scattering abilities of Al nanocrystals and the residual amorphous matrix, the value of which for  $\text{Al}_{88}\text{Ni}_4\text{Sm}_8$  alloy was found to be 0.37 [29].

## 2. Results and discussion thereof

Analysis of the diffraction patterns of these samples (Fig. 1) showed that the nanophase composite formed during the annealing process contains Al nanocrystals, the volume fraction of which is  $X_h = 0.05$ , the average size is  $L_h = 14\ \text{nm}$ , while deformation at room temperature leads to the formation of nanocrystals with an average size of 6 nm and a fraction of the crystallized volume  $X_d = 0.22$  [14]. The volume densities of nanocrystals ( $N = 6X / (\pi L^3)$ ) in the annealed and deformed samples calculated using these parameters are  $N_h = 3.48 \cdot 10^{22}\ \text{m}^{-3}$  and  $N_d = 1.95 \cdot 10^{24}\ \text{m}^{-3}$ , respectively. These characteristics were taken as reference, and the main task of the analysis was to develop an approach for estimating the values of the physical parameters included in the equations for the rates of crystal nucleation at which nanophase composites with the above mentioned structural parameters are formed during annealing and deformation.

The analysis of the nanocrystallization process in the present study was carried out under the assumption of a homogeneous (fluctuation) nucleation mechanism, the applicability of which was established in a number of works [19–22]. Due to the fact that nanocrystals of pure Al grow in the glass investigated (i.e., as the crystalline phase is formed, the composition of the parent (amorphous) phase is enriched with alloying elements), to describe the nucleation process, the classical equation [16] is used, which takes into account the effect of changing of concentration ( $C_M$ ) on the

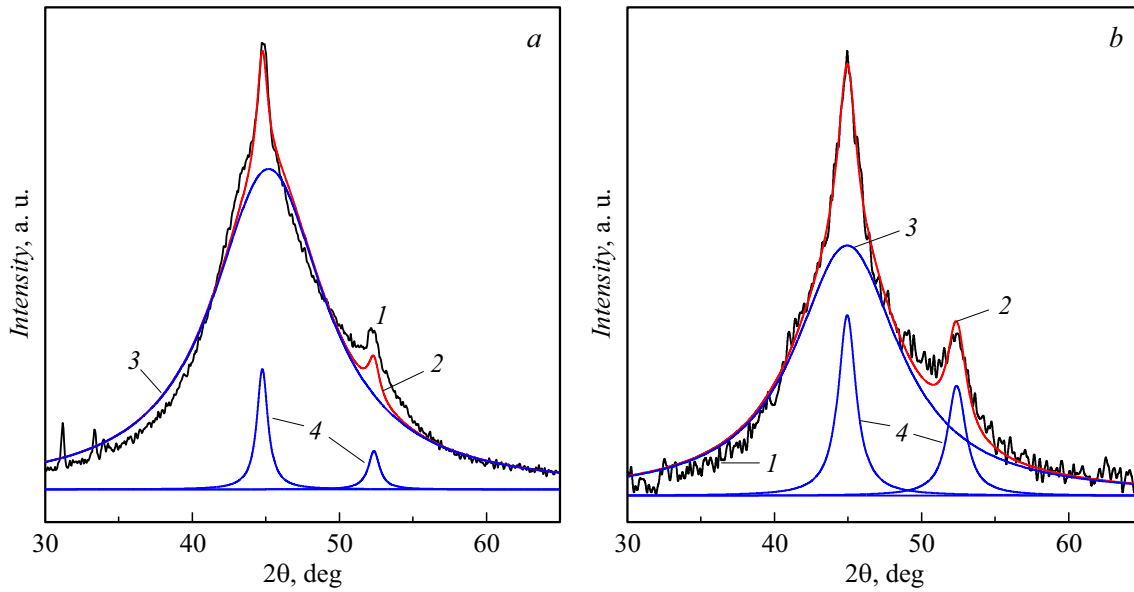


**Figure 1.** X-ray diffraction patterns of melt-quenched ribbons of the  $\text{Al}_{87}\text{Ni}_8\text{Gd}_5$  alloy after isothermal annealing for 1 h at 448 K (a) and after torsion by 1 turn under a pressure of 4 GPa (b): 1 — experimental spectrum, 2 — total curve, 3 — diffuse halo from the residual amorphous phase, 4 — the peaks (111) and (200) of Al nanocrystals.

work of formation of a critical nucleus in the form [22]

$$J(T, t) = \frac{N_0}{a_0^2} D(T) \exp \left[ -\frac{W^*}{T} \right] \\ = \frac{N_0}{a_0^2} D(T) \exp \left\{ -\frac{1\pi\sigma^3 V_m^2}{3kT\Delta G_c^2(T, C_M)} \right\}, \quad (3)$$

where  $W^*$  is the work for formation of a critical nucleus,  $N_0$  is the number of atoms per unit volume,  $a_0$  is the diffusion jump distance equal to the average atomic diameter,  $D(T)$  is the diffusivity controlling the transition of atoms across the interface,  $\sigma$  is the specific free energy of the nucleus–amorphous phase interface,  $V_m$  is the molar volume of amorphous phase,  $\Delta G(T, C_M)$  is the thermodynamic driving force for crystallization, and  $k$  is the Boltzmann constant. Changes in the thermodynamic driving force caused by changes in the composition of the matrix were taken into account within the framework of the model of regular solutions [30]:

$$\Delta G_c(T, C_M) = (T_m - T) \{ \Delta S + R \ln[1 - C_M(t)] \}, \quad (4)$$

where  $T_m$  is the current temperature,  $R$  is the universal gas constant, and  $\Delta S$  is the entropy jump during crystallization. Since nucleation in glasses occurs at deep undercoolings, the value of  $\Delta S$  was calculated using the developed for such a case approximate relationship [31]:

$$\Delta S = 2H_m T / [T_m(T_m + T)] \quad (5)$$

(where  $H_m$  is the melting heat at  $T_m$ ), which contains only two parameters and is widely used in the literature [30]. Changes in the matrix concentration caused by the formation of Al nanocrystals were calculated using equation (4),

which took into account the dynamics of changes in the fraction of crystallized volume [32]:

$$C_M(t) = C_1 - [C_1 - C_M^0] \times \exp(-3\alpha_H D t / r_S^2), \quad (6)$$

where  $C_M^0$  is the initial total concentration of alloying agents in the amorphous matrix ( $= 0.13$ ),  $C_1$  is the concentration of alloying agents at the boundary of a growing nanocrystal, taken as  $2C_M^0$ ,  $\alpha_H$  ( $\sim 1$ ) is the coefficient depending on the concentration of alloying elements in the nanocrystal, matrix and at the boundary,  $r_S$  is half of the average distance between growing crystallites, equals to  $0.5LX^{-1/3}$ .

In calculating the nucleation rate of  $J(T, t)$ , the parameters of pure Al ( $a_0 = 2.86 \cdot 10^{-10}$  m,  $T_m = 933.5$  K,  $\Delta H_m = 10784$  J/mol,  $N_0 = 3.02 \cdot 10^{28}$  m $^{-3}$ ,  $V_m = 1.08 \cdot 10^{-5}$  m $^3$ /mol), taken from the reference literature [33] used. The value of the effective diffusion coefficient  $D(T)$ , involved in equations (1) and (4), at annealing temperature of 448 K ( $12.8 \cdot 10^{-20}$  m $^2$ /s) was calculated from the empirical relationship  $D(T)$  [m $^2$ /s] =  $5.96 \cdot \exp(-20970/T)$ , obtained in the work [23] based on the results of the analysis of the nanocrystallization process of  $\text{Al}_{87}\text{Ni}_8\text{Gd}_5$  metallic glass, analyzed in the present study. Thus, from the set of parameters of equation (3), which determine the rate of nucleation of Al nanocrystals at 448 K in the glass being analyzed, the value of the specific free energy of the nucleus/matrix interface  $\sigma$  remains unknown. Due to the lack of adequate theoretical approaches for estimating  $\sigma$ , this value is usually considered as the model parameter [19,20,22] and its values are determined by fitting the calculated results to the experimentally measured ones. In this study, the value of  $\sigma$  at a temperature of

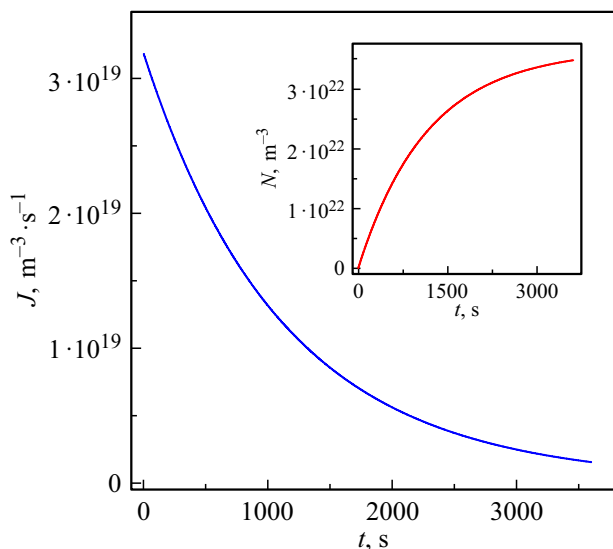


**Figure 2.** Changes in the nucleation rate and volume density (inset) of Al nanocrystals in metallic glass  $\text{Al}_{87}\text{Ni}_8\text{Gd}_5$  during isothermal annealing at 448 K, calculated using equation (3).

448 K was determined by fitting the value of the volume density of nanocrystals, calculated from the relationship

$$N(t) = \int_0^t J(t') [1 - X(t')] dt' \quad (7)$$

for  $t = 3600$  s, to the value of  $N_h = 3.48 \cdot 10^{22} \text{ m}^{-3}$  being estimated from the structural characterization of the heat-treated sample. Calculations have shown that the value  $N$  is very sensitive to the values  $\sigma$ , and almost complete agreement is achieved at  $\sigma = 0.0856(2) \text{ J/m}^2$ . The value  $\sigma$  obtained in this way is in good agreement with similar estimates of this parameter, which characterizes the rate of nucleation of Al nanocrystals in AlNiY amorphous alloys ( $0.07 \text{ J/m}^2$  [19]), ( $0.076 \text{ J/m}^2$  [20]) and ( $0.084 \text{ J/m}^2$  [22]).

Calculations using the above parameters also showed that during the formation of 5% Al nanocrystals, the total concentration of alloying elements in the residual amorphous matrix increases to 17.3 at.%, the thermodynamic driving force decreases from 3076 to 2869 J/mol, the work of formation of a critical nucleus ( $W^*$ ) increases from 9089 to 10450 K, and the nucleation rate decreases by more than an order of magnitude — from  $3.18 \cdot 10^{19}$  to  $1.54 \cdot 10^{18} \text{ m}^{-3} \text{ s}^{-1}$  (Fig. 2). As can be seen from Fig. 2, the volume density of nanocrystals increases along the curve with saturation, which is typical for the nanocrystallization process [6,20]. The calculated values of the nucleation rate of Al nanocrystals at 448 K in  $\text{Al}_{87}\text{Ni}_8\text{Gd}_5$  glass are consistent in order of magnitude with a similar estimate of  $J = 4 \cdot 10^{19} \text{ m}^{-3} \text{ s}^{-1}$  for  $\text{Al}_{88}\text{Y}_7\text{Fe}_5$  amorphous alloy at 460 K [21]. It should be also noted that calculations of the nucleation rates of Al nanocrystals in  $\text{Al}_{87}\text{Ni}_8\text{Y}_5$  amorphous alloy showed that as the fraction of crystallized volume

increased, the decrease in  $J(t)$  values could reach by 2–3 orders of magnitude [22].

The same shape of the size distributions of Al nanocrystals formed in the glass during heating and deformation by the HPT method [10], indicates the identity of the nanocrystallization mechanism. For this reason, to estimate the nucleation rate during deformation of glass  $\text{Al}_{87}\text{Ni}_8\text{Gd}_5$ , an approach similar to that described above was used. The main difference in the approach to the analysis of deformation-induced nanocrystallizing was the substitution into equation (3) of the value of the effective diffusion coefficient determined by the method described in the Refs. [24,25]. Substituting into the relation for parabolic growth  $D_D \sim r^2/t$  [26] the experimentally determined radius of the nanocrystal ( $r = L/2 = 3 \text{ nm}$ ), grown during the time ( $t = 60 \text{ s}$ ) of one revolution of the anvil, gives  $D_D = 1.5 \cdot 10^{-19} \text{ m}^2/\text{s}$ . The value of the effective diffusion coefficient, which governs the growth of Al nanocrystals, estimated in this way, is significantly lower than  $D_D \sim 10^{-16} \text{ m}^2/\text{s}$ , estimated from the growth of crystals of the solid solution of tin in copper [24], but close to the diffusion coefficient ( $10^{-20} - 10^{-19} \text{ m}^2/\text{s}$ ), which controls the initial stages of crystallization of metallic glasses based on Fe [25]. A comparison of the value  $D_D = 1.5 \cdot 10^{-19} \text{ m}^2/\text{s}$  with the above temperature dependence  $D(T)$  for the effective diffusion coefficient of the glass investigated from [23] shows that it corresponds to an effective deformation temperature equal to  $\approx 465 \text{ K}$ , which is consistent with the concept proposed in [27].

On the other hand, the summarized results of the experimental studies [34] give grounds to consider the formation of crystalline phases during of deformation as a mechanically induced effect. In this case, the deformation-stimulated mass transfer in equation (3) can be characterized by the value of the effective diffusion coefficient, while the values of the thermodynamic factor will correspond to room (300 K) temperature. When implementing this approach in this work, the fact was taken into account that the temperature dependence of the thermodynamic potential difference  $\Delta G(T)$ , described by both exact and a number of approximate models, has a maximum at some temperatures below  $T_m/2$  [18]. In particular, for the model used in the study (equations (4) and (5)), the temperature for maximum  $\Delta G$  for Al is at 387 K. Due to the fact that the decrease in the thermodynamic driving force with increasing of the deviation degree from equilibrium is physically incorrect, to analyze the processes occurring at temperatures below the maximum temperature, the maximum value  $\Delta G(T)$  is used. When substituting the value  $\Delta G(387)$  and temperature  $T = 300 \text{ K}$  into the second factor of equation (3), the value of the experimentally observed volume density Al nanocrystals in the deformed sample ( $1.95 \cdot 10^{24} \text{ m}^{-3}$ ) is achieved at the value  $\sigma = 0.0649(2) \text{ J/m}^2$ .

Compared to the isothermal case, the deformation-induced crystallization of  $\text{Al}_{87}\text{Ni}_8\text{Gd}_5$  glass leads to the formation of a significantly higher fraction of the crystalline phase (22%), a greater decrease of the difference of

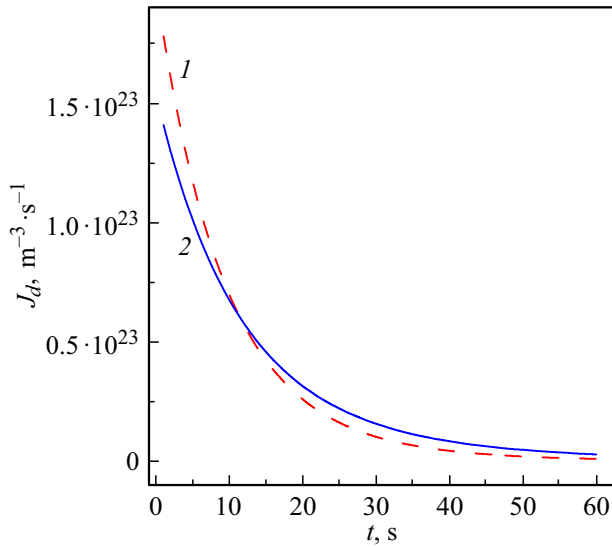


**Figure 3.** Variations in the rate of nucleation of Al nanocrystals during deformation, calculated without taking into account (dashed line) and taking into account the influence of pressure on the work for formation of a critical nucleus (solid line).

thermodynamic potentials (from 3056 to 2593 J/mol) and a significant increase of the work of formation of a critical nucleus (from 4000 to 5558 K). However, the absolute values  $W^*$  corresponding to a temperature of 300 K are almost two times lower than that at 448 K, which determines a higher nucleation rate compared to the isothermal process, which during deformation decreases by almost two orders of magnitude (from  $1.78 \cdot 10^{23}$  to  $9.94 \cdot 10^{20} \text{ m}^{-3} \cdot \text{s}^{-1}$  (curve 1 in Fig. 3)).

The estimated parameters of deformation-induced -crystallization, which are discussed below, seem physically reasonable, but this model does not take into account that the nucleation process in the amorphous phase occurs under applied external pressure, which in the present case was 4 GPa. From the results [35,36] published in the literature, it is known that pressure leads to a decrease in the thermal stability of the amorphous phase in Al-based glasses, but there is no quantitative analysis of the processes of nucleation and growth of nanocrystals in these studies. The difficulty of quantitative analysis is caused by the fact that pressure affects both the kinetic terms (diffusion coefficient) and the thermodynamic ones in the equations for nucleation and growth rates. In the approach proposed in the present study, the value of the diffusion coefficient is estimated independently from the average size of the nanocrystal; therefore, to assess the influence of pressure, it is necessary to evaluate its contribution to the work of formation of the critical nucleus. To do this, we use the relationship given in the study [36] for the work of formation of a critical nucleus

$$\Delta W^*(t, T, P) = \frac{16\pi\sigma^3}{3k} \left( \frac{V_m}{\Delta G(t, T)_c + P\Delta V} \right)^2, \quad (8)$$

within the framework of which an analysis was carried out of the deformation-induced crystallization of the amorphous alloy  $\text{Al}_{85}\text{Ce}_8\text{Ni}_5\text{Co}_2$  under HPT conditions and grinding in a ball mill. (Here  $V$  is applied pressure, and  $\Delta V$  is volume change associated with the formation of a crystalline Al nucleus). As in the study [36], to assess the effect of pressure on the nucleation rate, the value  $\Delta V/V_m$  was taken equal to 2%.

As follows from relation (8), taking into account pressure leads to an increase in the driving force of crystallization (by 856 J/mol), which, to obtain an experimentally determined volume density, is compensated by an increase in the specific free energy of the nucleus/matrix interface. Indeed, the density  $N_d = 1.95 \cdot 10^{24} \text{ m}^{-3}$  was achieved with the value  $\sigma = 0.0801(2) \text{ J/m}^2$ . At this value  $\sigma$ , the work of formation of a critical nucleus increased from 4072 to 5238 K, and the nucleation rate during deformation decreased from  $1.41 \cdot 10^{23}$  to  $2.88 \cdot 10^{21} \text{ m}^{-3} \cdot \text{s}^{-1}$  (curve 2 in Fig. 3). As can be seen from the figure, the rate of nucleation of Al nanocrystals under pressure changes more smoothly, which is due to a higher specific surface energy.

Both values  $\sigma$  estimated for the nucleation process under deformation conditions, related to room temperature, are lower than that for the nucleation rate at a temperature of 448 K. This result is qualitatively consistent with the classical theory of crystallization, in which the specific free energy of the nucleus/melt interface is assumed to be a linearly increasing function of temperature [37]. Therefore, it seems interesting to compare the dependences  $\sigma(T)$  for  $\text{Al}_{87}\text{Ni}_8\text{Gd}_5$  glass calculated using the above values with the data and estimates available in the literature. In analytical form, the temperature dependence of the specific surface energy for the case of deformation-induced crystallization without taking into account the influence of pressure on the work of formation of a critical nucleus has the form  $\sigma(T) = 0.0229 + 1.4 \cdot 10^{-4} T \text{ [J/m}^2\text{]}$ , and taking into account the influence of pressure may be written as  $\sigma(T) = 0.0688 + 3.76 \cdot 10^{-5} T \text{ [J/m}^2\text{]}$ . In Fig. 4, these dependences (1 and 2, respectively) are compared with the dependence  $\sigma(T) = 0.058 + 6.69 \cdot 10^{-5} T \text{ [J/m}^2\text{]}$  [36] calculated for the nucleation of Al nanocrystals in  $\text{Al}_{85}\text{Ce}_8\text{Ni}_5\text{Co}_2$  glass according to the approximate model [38]. If, as a criterion for the correctness of the given dependencies, to use the value of the parameter  $\sigma = 0.108 \text{ J/m}^2$ , determined from experimental studies of the nucleation of Al crystals in a melt at the melting temperature, then the most correct relation is 2, which gives the value  $0.104 \text{ J/m}^2$ , while the expressions 1 and 3 give values of  $0.153$  and  $0.12 \text{ J/m}^2$  (Fig. 4). Note also that the slope of the linear dependence  $\sigma(T)$  for the case of deformation-induced crystallization at atmospheric pressure ( $1.4 \cdot 10^{-4} \text{ J/(m}^2 \cdot \text{K)}$ ) is noticeably higher than the values of this parameter given in the literature for  $\text{Ti}_2\text{Ni}$  glass ( $6.4 \cdot 10^{-5} \text{ J/(m}^2 \cdot \text{K)}$ ) [39] and mercury ( $(5-9) \cdot 10^{-5} \text{ J/(m}^2 \cdot \text{K)}$ ) [37].



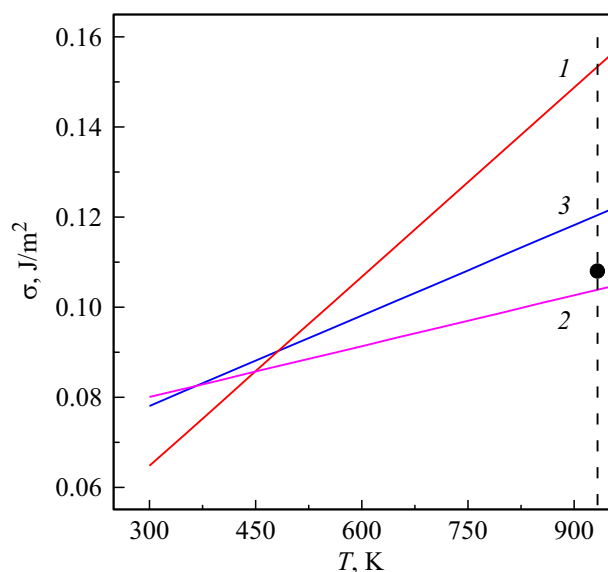


**Figure 4.** Temperature dependences of the specific free energy of the nucleus/amorphous phase interface: 1, 2 — for glass  $\text{Al}_{87}\text{Ni}_8\text{Gd}_5$  for the case of crystallization at atmospheric and applied external pressure, respectively, 3 — data [36] for  $\text{Al}_{85}\text{Ce}_8\text{Ni}_5\text{Co}_2$  glass. The dot indicates the value  $I\sigma = 0.108 \text{ J/m}^2$  estimated from experimental data for pure Al [18] at the melting temperature shown by the vertical dashed line.

## Conclusion

To describe variations in the rate of crystal nucleation in the amorphous phase under severe plastic deformation, an analytical model is proposed for the first time using the coefficient of deformation-stimulated diffusion in combination with the work of formation of a critical nucleus at room temperature. Using as example of analysis of the nanocrystallization process in  $\text{Al}_{87}\text{Ni}_8\text{Gd}_5$  metallic glass under conditions of isothermal annealing and severe plastic deformation, it was established that the proposed approach correctly describes the experimentally observed higher volume density of Al nanocrystals in the deformed sample ( $1.95 \cdot 10^{24} \text{ m}^{-3}$ ) compared to the heat-treated one ( $3.48 \cdot 10^{22} \text{ m}^{-3}$ ). The estimated values of the thermodynamic and kinetic parameters of the classical equation for the rate of homogeneous nucleation under isothermal conditions and during the deformation process, taking into account the contribution of the applied holding pressure, are physically reasonable, which opens up the possibility of using the proposed approach to develop methods for controlling the process of deformation-induced nanocrystallization.

## Conflict of interest

The authors declare that they have no conflict of interest.

## References

- [1] Y. Yoshizawa, S. Oguma, K. Yamauchi. *J. Appl. Phys.*, **64** (10), 6044 (1988). DOI: 10.1063/1.342149
- [2] Y.-H. Kim, A. Inoue, T. Masumoto. *Mater. Trans. JIM*, **31** (8), 747 (1990). DOI: 10.2320/matertrans1989.31.747
- [3] H. Chen, Y. He, G.J. Shiflet, S.J. Poon. *Scr. Met. Mater.*, **25** (6), 1421 (1991). DOI: 10.1016/0956-716X(91)90426-2
- [4] H. Chen, Y. He, G.J. Shiflet, S.J. Poon. *Nature*, **367**, 541 (1994). DOI: 10.1038/367541a0
- [5] G. Abrosimova, D. Matveev, E. Pershina, A. Aronin. *Mater. Lett.*, **183**, 131 (2016). DOI: 10.1016/j.matlet.2016.07.053
- [6] M.A. Munoz-Morris, S. Surinach, L.K. Varga, M.D. Baro, D.G. Morris. *Scr. Mater.*, **47**, 31 (2002). DOI: 10.1016/S1359-6462(02)00093-3
- [7] A.M. Glezer, I.E. Permyakova, V.E. Gromov, V.V. Kovalenko. *Mechanical behavior of amorphous alloys* (SibGIU, Novokuznetsk, 2006)
- [8] E.A. Sviridova, S.G. Rassolov, V.V. Maksimov, V.I. Tkatch, V.K. Nosenko. *Physics Solid State*, **56** (7), 1355 (2014). DOI: 10.1134/S1063783414070312
- [9] Y.B. Wang, D.D. Qu, X.H. Wang, Y. Cao, X.Z. Liao, M. Kawasaki, S.P. Ringer, Z.W. Shan, T.G. Langdon, J. Shen. *Acta Mater.*, **60** (1), 253 (2012). DOI: 10.1016/j.actamat.2011.09.026
- [10] S.V. Vasiliev, A.I. Limanovskii, V.M. Tkachenko, T.V. Tsvetkov, K.A. Svyrydova, V.V. Burkhovetskii, V.N. Sayapin, O.A. Namuchuk, A.S. Aronin, V.I. Tkatch. *Mater. Sci. Eng. A*, **850**, 143420 (2022). DOI: 10.1016/j.msea.2022.143420
- [11] Z.Q. Ren, A.A. Churakova, X. Wang, S. Goel, S.N. Liu, Z.S. You, Y. Liu, S. Lan, D.V. Gunderov, J.T. Wang, R.Z. Valiev. *Mater. Sci. Eng. A*, **803**, 140485 (2020). DOI: 10.1016/j.msea.2020.140485
- [12] D.V. Gunderov, E.V. Boltynjuk, V.D. Sittikov, G.E. Abrosimova, A.A. Churakova, A.R. Kilmametov, R.Z. Valiev. *IOP Conf. Ser.: J. Phys.: Conf. Ser.*, **1134** (1), 012010 (2018). DOI: 10.1088/1742-6596/1134/1/012010
- [13] N. Boucharat, R. Hebert, H. Rösner, R. Valiev, G. Wilde. *Scr. Mater.*, **53** (7), 823 (2005). DOI: 10.1016/j.scriptamat.2005.06.004
- [14] A. Aronin, A. Budchenko, D. Matveev, E. Pershina, V. Tkatch, G. Abrosimova. *Rev. Adv. Mater.*, **46**, 53 (2016).
- [15] S.V. Vasiliev, T.V. Tsvetkov, K.A. Svyrydova, V.M. Tkachenko, A.S. Aronin, V.I. Tkatch. *J. Non-Cryst. Sol.*, **699**, 121968 (2023). DOI: 10.1016/j.jnoncrsol.2022.121968
- [16] J. Christian. *Teoriya prevrashcheniy v metallakh i splavakh (in Russian)* (Mir, M., 1978), part 1.
- [17] W. Koester, W. Herold. *Metal glasses* (Mir, M., 1983), p. 325–371.
- [18] K.F. Kelton. *Solid State Phys. — Advances in Research and Application*, eds. H. Ehrenreich, D. Turnbull (Acad. Press, NY., 1991), p. 75–177.
- [19] K.F. Kelton, T.K. Croat, A.K. Gangopadhyay, L.-Q. Xing, A.L. Greer, M. Weyland, X. Li, K. Rajan. *J. Non-Cryst. Sol.*, **317**, 71 (2003). DOI: 10.1016/S0022-3093(02)02004-5
- [20] X.Y. Jiang, Z.C. Zhong, A.L. Greer. *Mater. Sci. Eng. A*, **226–228**, 789 (1997). DOI: 10.1016/S0921-5093(96)10732-2
- [21] J.H. Perepezko, S.D. Imhoff, R.J. Hebert. *J. Alloys Comps.*, **495** (2), 360 (2010). DOI: 10.1016/j.jallcom.2009.10.051
- [22] S.G. Rassolov, V.V. Maksimov, T.N. Moiseeva, V.K. Nosenko, V.I. Tkatch. *Metallofiz. Noveishie Tekhnol.* **34**, (12), 1625 (2012)(in Russian).

- [23] V.I. Tkatch, S.G. Rassolov, V.K. Nosenko, V.V. Maksimov, T.N. Moiseeva, K.A. Svyrydova. *J. Non-Cryst. Sol.*, **358** (20), 2727 (2012). DOI: 10.1016/j.jnoncrysol.2012.02.023
- [24] B.B. Straumal, A.R. Kilmametov, I.A. Mazilkin, A. Korneva, P. Zemba, B. Baretzki. *Pis'ma v ZhETF*, **110** (9), 622 (2019) (in Russian). DOI: 10.1134/S0370274X1921010
- [25] I.E. Permyakova, A.M. Glezer, A.I. Kovalev, V.O. Vakhrushev. *Pis'ma v ZhETF*, **113** (7), 468 (2021) (in Russian). DOI: 10.31857/S1234567821070089
- [26] C. Zener. *J. Appl. Phys.*, **20**, 950 (1949). DOI: 10.1063/1.1698258
- [27] B.B. Straumal, A.A. Mazilkin, S.G. Protasova, A.R. Kilmametov, A.V. Druzhinin, B. Baretzki. *Pis'ma v ZhETF*, **112** (1), 45 (2020) (in Russian). DOI: 10.31857/S1234567820130078
- [28] A.A. Rusakov. *Rentgenografiya metallov* (Atomizdat, M., 1977) (in Russian).
- [29] T. Gloriant, M. Gich, S. Surinach, M.D. Baro, A.L. Greer. *Mater. Sci. Forum*, **343–436**, 365 (2000). DOI: 10.4028/www.scientific.net/MSF343-346.365
- [30] C.V. Thompson, F. Spaepen. *Acta Metall.*, **31** (12), 2021 (1983). DOI:10.1016/0001-6160(83)90019-6
- [31] C.V. Thompson, F. Spaepen. *Acta Metall.*, **22** (12), 1855 (1979). DOI: 10.1016/0001-6160(79)90076-2
- [32] V.I. Tkatch, S.G. Rassolov, T.N. Moiseeva, V.V. Popov. *J. Non-Cryst. Sol.*, **351**, 1658 (2005). DOI: 10.1016/j.jnoncrysol.2005.04.057
- [33] G.V. Samsonov. *Svoystva elementov. (Spravochnik)* (Metalurgiya, M., 1976) Part 1. (in Russian)
- [34] W.H. Jiang, M. Atzmon. *Acta Mater.*, **51**, 4095 (2003). DOI: 10.1016/S1359-6454(03)00229-5
- [35] F. Ye, K. Lu. *Acta Mater.*, **47** (8), 2449 (1999). DOI: 10.1016/S1359-6454(99)00104-4
- [36] P. Henits, A. Revesz, L.K. Varga, Zs. Kovacz. *Intermetallics*, **19**, 267 (2011). DOI: 10.1016/j.intermet.2010.10.007
- [37] F. Spaepen. *Solid State Phys. — Advances in Research and Application* (Acad. Press., NY, 1994), p. 1–32.
- [38] M. Palumbo, C. Papandrea, L. Battezzati. *J. Mater. Sci.*, **40**, 2431 (2005). DOI: 10.1007/s10853-005-1970-3
- [39] A.L. Greer. *Mater. Sci. Eng. A*, **179/180**, 41 (1994). DOI: 10.1016/0921-5093(94)90161-9

*Translated by V.Prokhorov*

*Translated by 123*